Universidade de Lisboa

Faculdade de Farmácia

Development of a capillary electrophoresis method for quantification of orally disintegrating tablets of nebivolol hydrochloride

Catarina Vasco Gonçalves Esteves

Trabalho de Campo orientado pela Professora Doutora Francesca Maestrelli, Professora Associada, Università degli Studi di Firenze e coorientado pela Professora Doutora Eduarda Mendes, Professora Auxiliar, da Faculdade de Farmácia da Universidade de Lisboa

Mestrado Integrado em Ciências Farmacêuticas

2023

Universidade de Lisboa

Faculdade de Farmácia

Development of a capillary electrophoresis method for quantification of orally disintegrating tablets of nebivolol hydrochloride

Catarina Vasco Gonçalves Esteves

Trabalho Final de Mestrado Integrado em Ciências Farmacêuticas apresentado à Universidade de Lisboa através da Faculdade de Farmácia

Trabalho de Campo orientado pela Professora Doutora Francesca Maestrelli, Professora Associada, Università degli Studi di Firenze e coorientado pela Professora Doutora Eduarda Mendes, Professora Auxiliar, da Faculdade de Farmácia da Universidade de Lisboa

2023

Resumo

Com o objetivo de quantificar o cloridrato de nebivolol em comprimidos de desintegração oral, no presente trabalho foi desenvolvido um método de eletroforese capilar. A gestão do conhecimento foi efetuada através da realização de experiências preliminares de exploração que incluíram a seleção de um ponto de partida adequado para a milimolaridade e o pH do tampão, bem como o comprimento adequado do capilar e a configuração da separação. Os melhores resultados foram obtidos com um tampão Britton-Robinson 30mM pH 2, utilizando a injeção *short-end* e pré-condicionamento ácido, a 22°C e voltagem de separação de -30kV. A deteção das amostras foi efetuada a 194nm. O cloridrato de procaína foi selecionado como padrão interno. Após a definição do sistema de separação fundamental, foi efetuada uma avaliação dos riscos e foram selecionados como parâmetros críticos do método, a voltagem de separação, a concentração do tampão e o pH do tampão. Para a otimização do método, os atributos críticos do método foram identificados como tempo de análise, eficiência dos picos de procaína e nebivolol, e resolução. A Metodologia de Superfície de Resposta, utilizando o *Face Centered Central Composite Design*, e o Método de Monte Carlo, permitiram a definição do Desenho da Região Operável do Método: tampão fosfato 27-35 mM pH 2.4-2.7; voltagem, -19 – -22 kV. As condições de ponto de trabalho totalmente otimizadas foram um tampão H_3PO_4 30mM pH 2.6; capilar, 33.0cm (8.5cm de comprimento efetivo) 50µm de diâmetro interno; voltagem, -21kV; temperatura, 22°C e injeção *short-end*, -50mbar x 5s + tampão -50mbar x 5s. Foi efetuado um estudo de robustez, utilizando o desenho Plackett-Burman, em torno do ponto ótimo, que sublinhou a necessidade de controlar as concentrações das espécies iónicas durante a preparação do tampão.

A validação do método foi efetuada de acordo com a diretriz Q2(R2) do Conselho Internacional para Harmonização. O Limite de Deteção, 0.0003 mg/mL, e o Limite de Quantificação, 0.0005 mg/mL, foram estimados com base nas suas relações sinal-ruído. Foram avaliadas a Seletividade, a Exatidão e a Precisão, bem como a Linearidade, avaliada utilizando oito concentrações diferentes de cloridrato de nebivolol, num intervalo de 0.0005 – 1.2000 mg/mL.

Palavras-chave: eletroforese capilar; cloridrato de nebivolol; desenvolvimento de método; desenho experimental; *quality by design*.

Abstract

In order to quantificate orally disintegrating tablets of nebivolol hydrochloride, a capillary electrophoresis method was developed in the present work. Knowledge Management was undertaken by running preliminary scouting experiments that encompassed the selection of a suitable starting point for separation buffer millimolarity and pH, and proper capillary length and separation setup. The best results were obtained for a 30 mM pH 2 Britton-Robinson buffer, using short-end injection and acidic pre-conditioning, at 22°C and -30 kV separation voltage. Sample detection was carried out at 194 nm. Procaine hydrochloride was chosen as internal standard. After defining the fundamental separation system, risk assessment was carried out, and Critical Methods Parameters were selected as separation voltage, buffer concentration, and buffer pH.

For the Method Optimisation, the Critical Method Attributes were identified as analysis time, efficiency of the peaks of procaine and nebivolol, and resolution. Response Surface Methodology, using Face Centered Central Composite Design, and Monte Carlo Simulations, allowed the definition of the Method Operable Design Region: 27–35 mM phosphate buffer pH 2.4–2.7; voltage, -19 – -22 kV. The fully optimized working point conditions were a H_3PO_4 30 mM pH 2.6 buffer; capillary, 33.0 cm (8.5 cm effective length) 50µm Internal Diameter; voltage, -21 kV; temperature, 22°C and short-end injection, -50 mbar x 5s + BGE -50 mbar x 5s. A robustness study, using Plackett-Burman design, was carried out around the optimal point, and it underscored the necessity to meticulously regulate the concentrations of the ionic species during buffer preparation.

Method Validation was performed according to International Council for Harmonisation Guideline Q2(R2). Limit of Detection, 0.0003 mg/mL, and Limit of Quantification, 0.0005 mg/mL, were estimated based on their signal-to-noise ratios. Selectivity, Accuracy and Precision were evaluated, as well as Linearity, evaluated using eight different concentrations of nebivolol hydrochloride, in a range of 0.0005 - 1.2000 mg/mL.

Keywords: capillary electrophoresis; nebivolol hydrochloride; method development; experimental design; quality by design.

Acknowledgments

This thesis would not have been possible without the guidance and the help of various individuals, to whom I would like to express my sincere appreciation.

I am deeply grateful to my supervisor, Professor Francesca Maestrelli, for the guidance and assistance in every stage of the research project at Università degli Studi di Firenze. My deep gratitude also extends to my co-supervisor, Professor Eduarda Mendes, for always being available to help me and for the constructive suggestions.

I am indebted to Luca Marzullo, for all the patience and invaluable advice, in and out of the laboratory, for sharing his in-depth knowledge and for being a constant support throughout the entire journey of this project. I am also thankful for my partner in the laboratory, Rebeca, for all the emotional support and all the fun we had while working together.

I would like to express my gratitude to those who have walked with me on this challenging but fulfilling journey.

To FFUL, for being my second home during the past five years and to AEFFUL for shaping the person I am today.

To my dearest friends, Manuel, Beatriz, Inês, Miguel, Gabriel, Diogo, Maria, Catarina, and Sofia, for always being there for me and for your unconditional friendship. To my pets, Saphira and Ruby, for their companionship and for bringing comfort and joy to my days.

To my partner and best friend, Pasquali, for being my safe harbour. Your support was my strength.

To my grandparents, João, Isaura and Alice, for always believing in me. To my grandfather Fernando, for always being my biggest cheerleader.

To my brother, Afonso, for inspiring me every day and always having the kindest words.

To my parents, Carla and João, whose constant encouragement fueled my perseverance. Thank you for being my pillars, this achievement is as much yours as it is mine.

Abbreviations

API	Active Pharmaceutical Ingredient
AQbD	Analytical Quality by Design
ATP	Analytical Target Profile
BGE	Background Electrolyte
CE	Capillary Electrophoresis
CCD	Central Composite Design
CMA	Critical Method Attribute
CMP	Critical Methods Parameter
CZE	Capillary Zone Electrophoresis
DoE	Design of Experiments
EOF	Electroosmotic Flow
I.D.	Inner Diameter
IS	Internal Standard
LOD	Limit Of Detection
LOQ	Limit Of Quantification
MODR	Method Operable Design Region
NEB	Nebivolol Hydrochloride
O.D.	Outer Diameter
ODT	Orally Disintegrating Tablets
PAR	Peak Area Ratio
PBD	Plackett-Burman Design
PRO	Procaine Hydrochloride
QbD	Quality by Design
RSD	Relative Standard Deviation

RSM	Response Surface Methodology
SD	Standard Deviation
S/N	Signal-to-Noise
TCAR	Time-Corrected Area Ratio
UV	Ultraviolet

Table of contents:

Table of Figures:

List of Tables:

1 Introduction

1.1 Aim of the Project

This work was developed under the Erasmus+ Programme, at the Scuola di Scienze della Salute Umana, Università degli Studi di Firenze, in Florence, Italy, between the months of January and April of 2023. The aim of the project was the development of a method to quantify orally disintegrating tablets (ODT) of nebivolol hydrochloride.

The project was already ongoing and as a result some studies had already been conducted. The full project was focused on the development of oral solid dosage forms of nebivolol hydrochloride with improved solubility and dissolution properties. NEB was taken as a model drug (representative substance) because of its well-understood pharmacological properties and due to its low dissolution rate, low bioavailability, low wettability, and low water solubility. Orally disintegrating tablets were formulated using different excipients and compositions, to obtain a complete drug dissolution within a few minutes in the mouth. Among the different excipients tested during the ODT formulation, it was employed an excipient, GalenIQ 721. When trying to quantify the prepared ODT of nebivolol hydrochloride, it was observed the overlapping of Nebivolol and GaleniIQ UV signals in High performance liquid chromatography (HPLC) and so the dosage could not be exactly confirmed.

As it would be necessary to quantify the drug across various tablet formulations and tailored to different purposes (routine content uniformity analysis, dissolution studies and accelerated degradation studies), the development of another method of quantification was imperative. The goal was to achieve baseline separation of nebivolol and the internal standard chosen, while ensuring they remained distinct from any possible overlapping excipient peaks, such as GalenIQ 721.

Thus, to address the challenge experienced, it was decided to develop a Capillary Electrophoresis quantification method.

1.2 Capillary Electrophoresis

1.2.1 Principles

Capillary electrophoresis (CE) is a physical method of analysis with high efficiency. This analytical method is used most predominantly because it gives faster results and provides high resolution separation. CE is based on the migration, inside a capillary, of charged analytes dissolved in an electrolyte solution, under the influence of a direct-current electric field (1,2).

The velocity of this migration is influenced by several factors, including the intensity of the electric field (E), the electrophoretic mobility of the analyte and the electro-osmotic mobility of the buffer inside the capillary (3).

The electrophoretic mobility of a solute (μ_{ep}) depends on the characteristics of the solute (electric charge, molecular size and shape) and those of the buffer in which the migration occurs (type and ionic strength of the electrolyte, pH, viscosity and additives) (3). The electrophoretic velocity (v_{ep}) of a solute, is given by equation 1.

$$v_{ep} = \mu_{ep} \times E = \left(\frac{q}{6\pi\eta r}\right) \times \left(\frac{V}{L}\right) \qquad (1)$$

Where, q = effective charge of the solute; η = viscosity of the electrolyte solution; r = Stoke's radius of the solute; V = applied voltage; L = total length of the capillary.

In addition to electrophoretic migration, another factor to have in mind is electroosmosis, which originates at the capillary wall and gives rise to the electroosmotic flow (EOF). The inner surface of the silica wall exposes acidic silanol groups which, ionized as SiO^- at pH values higher than 2, interact electrostatically with the buffer cations, which are attracted, some firmly, some loosely, by the wall charges. The application of a high potential along the capillary induces the migration of the loosely bound cations towards the cathode, which is typically in the direction of the detector (4,5). This migration drags water osmotically in the same direction, creating a relevant flow of liquid known as the EOF, depicted in Fig. 1.

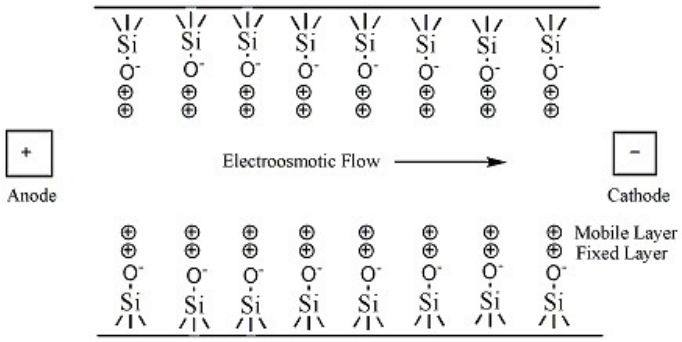

Figure 1: Depiction of the interior of a fused-silica gel capillary in the presence of a buffer solution.

The velocity of the EOF depends on the electroosmotic mobility (μ_{eo}) which, in turn, is determined by the charge density on the capillary internal wall and the buffer characteristics (3). The electroosmotic velocity (v_{eo}) is given by equation 2.

$$v_{eo} = \mu_{eo} \times E = \left(\frac{\varepsilon\zeta}{\eta}\right) \times \left(\frac{V}{L}\right) \qquad (2)$$

Where ε = dielectric constant of the buffer; ζ = zeta potential of the capillary surface.

The velocity of the solute (v) is given by equation 3.

$$v = v_{ep} \times v_{eo} \qquad (3)$$

In normal capillary electrophoresis, anions will migrate in the opposite direction of the EOF and their velocities will be smaller than the EOF velocity. Conversely, cations will migrate in the same direction as the EOF and their velocities will be greater than the EOF velocity (3), as represented in Fig. 2.

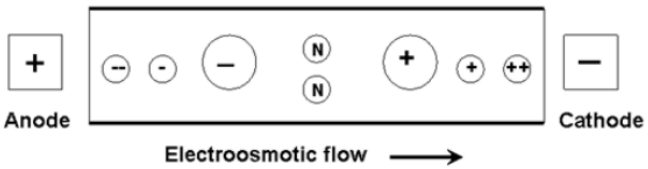

Figure 2: Effect of the electroosmotic flow and electrophoretic mobility on charged and neutral analytes migration (6).

CE detectors transmit the peaks corresponding to the compounds under analysis to the software. The peak's identification is possible due to its different migration time.

The time (t) taken by the solute to migrate the distance (l) from the injection end of the capillary to the detection point is called migration time and is given by equation 4.

$$t = \frac{l}{v_{ep} + v_{eo}} = \frac{l \times L}{(\mu_{ep} + \mu_{eo}) \times V} \qquad (4)$$

Following the introduction of the sample into the capillary, each analyte ion of the sample migrates within the background electrolyte as an independent zone, according to its electrophoretic mobility. The difference necessary to resolve two zones relies both on the width of the zones and their difference in migration time (1,3).

Zone width is strongly dependent on the zone dispersion processes that act on it and this dispersion should be controlled to avoid an increased zone width and the mobility difference necessary to achieve separation. Under ideal conditions the sole contribution to the solute-zone broadening is molecular diffusion of the solute along the capillary (longitudinal diffusion) (1,3). In this ideal case the efficiency of the zone, expressed as the number of theoretical plates (N), is given by equation 5.

$$N = \frac{(\mu_{ep} + \mu_{eo}) \times V \times l}{2 \times D \times L} \qquad (5)$$

Where D = molecular diffusion coefficient of the solute in the buffer.

In practice, other phenomena can also significantly contribute to band dispersion, namely: heat dissipation (Joule heating), that leads to radial temperature gradients and parabolic flow velocity profiles; sample adsorption onto the capillary wall, that usually causes severe peak tailing; mismatched conductivity between sample and buffer, where solutes with higher conductivities than the running buffer result in fronted peaks and solutes with lower conductivities than the running buffer result in tailed peaks; length of injection zone, as injection lengths should be less than the diffusion-controlled zone length; detector cell size, that should be small relative to peak width; and unlevelled buffer reservoirs, that generate laminar flow (1,3).

Regarding the separation between two bands (expressed as the resolution, R_s), it can be obtained by modifying the electrophoretic mobility of the analytes, the electroosmotic mobility induced in the capillary and by increasing the efficiency of the peaks of each analyte (3), according to equation 6.

$$R_s = \frac{\sqrt{N}\left(\mu_{epb} - \mu_{epa}\right)}{4\left(\bar{\mu}_{ep} + \mu_{eo}\right)} \qquad (6)$$

Where μ_{epb} and μ_{epa} = electrophoretic mobilities of the two analytes separated; $\bar{\mu}_{ep}$= mean electrophoretic mobility of the two analytes = ½ ($\mu_{epb} + \mu_{epa}$).

1.2.2 Instrumentation

An apparatus for capillary electrophoresis is schematized in Fig. 3 and it is composed of: a high-voltage, controllable direct-current power supply; buffer reservoirs, held at the same level, containing the prescribed anodic and cathodic solutions; electrode assemblies (the cathode and the anode), immersed in the buffer reservoirs and connected to the power supply; a separation capillary (usually made of fused-silica) which, when used with some specific types of detectors, has an optical viewing window aligned with the detector. The ends of the capillary are placed in the buffer reservoirs; a suitable injection system; a detector able to monitor the amount of substances of interest passing through a segment of the separation capillary at a given time; it is usually based on absorption spectrophotometry - ultraviolet (UV) and visible - or

fluorimetry; a thermostatic system able to maintain a constant temperature inside the capillary is recommended to obtain a good separation reproducibility; a recorder and a suitable integrator or a computer (3,5).

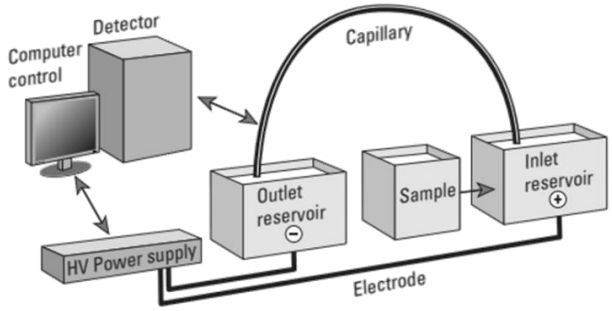

Figure 3: Simplified scheme of capillary electrophoresis instrumentation (5).

1.2.3 Modes of Operation

The versatility of CE is derived from its numerous modes of operation. Using the same CE instrumental hardware, several separation modes can be carried out, based on different physical-chemical principles, and they offer the analyst a variety of ways to approach an analytical problem (1).

In short, the modes of operation available are: capillary zone electrophoresis (CZE), micellar electrokinetic chromatography, capillary electrochromatography, capillary isoelectric focusing, capillary gel electrophoresis and capillary isotachophoresis. CZE is the most widespread mode of CE, and it has been used for analytes as diverse as sodium ions, drugs, and protein molecules (5).

1.2.3.1 Capillary Zone Electrophoresis

In capillary zone electrophoresis, analytes are separated in a capillary containing only buffer without any anticonvective medium. With this technique, separation is achieved as solutes migrate at different velocities and in discrete zones. Using this mode, the analysis of both small ($M_r < 2000$) and large molecules ($2000 < M_r < 100\,000$) can be accomplished. Moreover, the high efficiency achieved in capillary zone electrophoresis

enables the separation of molecules having only minute differences in their charge-to-mass ratio (1,3,7).

1.2.4 Optimization

It is essential for CZE to have control over the electrophoretic mobility of the solutes and over the EOF. In order to optimize and control separation, the time of analysis, the order of separation and reproducibility of separation are crucial parameters for the overall method. Optimization of the separation is a complex process, involving the consideration of various separation parameters. The main factors to be taken into account when developing separations are parameters related to the instrumentation and electrolytic solution (8).

1.2.4.1 Instrumental parameters

Although separation time is inversely proportional to applied voltage, with increasing voltage, the temperature will rise due to an excessive heat production, causing viscosity gradients in the buffer inside the capillary. This effect causes band broadening and decreases resolution, where it is observed a reduction in efficiency and/or a disproportionate, non-linear increase in EOF or solute mobility. Stable regulation of the voltage (± 0.1 %) is required to maintain high migration time reproducibility (1).

Another parameter is electrode polarity, which can be normal (anode at the inlet and cathode at the outlet) or reversed. In normal polarity the EOF will move toward the cathode. If the electrode polarity is reversed, the EOF is away from the outlet and only charged analytes with electrophoretic mobilities greater than the EOF will pass to the outlet (5).

Regarding temperature, its increase depends on the power (product of voltage and current) generated and is determined by the capillary dimensions, thermal conductivity of the buffer, and the applied voltage. Significantly elevated temperatures will result when the power generation exceeds dissipation and, while the absolute rise in temperature is generally not detrimental (even though in some cases, an increase in capillary temperature can cause a conformational change in proteins, modifying their migration time and the efficiency of the separation), temperature gradients are. Thermal

dissipation of the heat through the capillary walls can result in higher temperatures in the center than at the wall. These temperature gradients cause buffer viscosity differences and give rise to zone deformation. Control of temperature differentials is critical since a one degree change in temperature results in a 2 to 3 % change in viscosity (and therefore a 2 to 3 % change in migration velocity) (1).

When it comes to the capillary, both length and internal diameter dimensions contribute to analysis time, efficiency of separations and load capacity. Increasing both effective length (from the point of injection to the point of detection) and total length can decrease the electric fields (working at constant voltage) which increases migration time. By reducing the capillary inner diameter and therefore the electric current, a decrease in temperature differences can also be realized (1).

1.2.4.2 Electrolytic solution parameters

In CZE, the whole system is filled with a background electrolyte (BGE), whose primary functions are to provide the transport of electric current, as well as to maintain constant conditions for the analyte ions during the separation, and to make these conditions independent of the sample composition (9). To allow electric current to pass through the solution when a voltage is applied, the BGE must contain charged particles.

Since water electrolysis takes place at both the electrodes: at the anode protons and oxygen, at the cathode hydrogen and hydroxide ions are produced, without a buffer solution, the pH in the inlet and the outlet vials would change as soon as power supply was switched on. Thus, BGE should always be a buffering salt, whose buffering capacity should be sufficient to avoid pH changes during the analysis or between analyses, in the pH range of choice (5).

That being said, the running buffer selection is extremely important to the success of the CE separation. Effective buffer systems have a range of approximately one pH unit centered around their pKa value (for example, a buffer with a pKa of 7 would be usable from pH 6.0 to pH 8.0 (2,4). Besides having a good buffering capacity in the pH range of choice, a buffer for use in CE should also possess low absorbance at the wavelength of detection of the sample and low mobility, to minimize current generation (that is, large, minimally-charged ions) (10).

Commonly used buffers and their useful pH ranges can be seen in Table 1.

Table 1: Commonly used buffers (1).

Name	pK_a	Name	pK_a
Phosphate	2.12 (pK_{a1})	Phosphate	7.21 (pK_{a2})
Citrate	3.06 (pK_{a1})	TES	7.50
Formate	3.75	HEPES	7.55
Succinate	4.19 (pK_{a1})	TRICINE	8.00
Citrate	4.74 (pK_{a2})	Glycine amide, hydrochloride	8.20
Acetate	4.75	Glycylglycine	8.25
Citrate	5.40 (pK_{a3})	TRIS	8.30
Succinate	5.57 (pK_{a2})	BICINE	8.35
MES	6.15	Morpholine	8.49
ADA	6.60	Borate	9.24 (pK_{a1})
BIS-TRIS propane	6.80	CHES	9.50
PIPES	6.80	CHAPSO	9.60
ACES	6.90	CAPS	10.40
MOPSO	6.90	Phosphate	12.32 (pK_{a3})
Imidazole	7.00	Borate	12.40 (pK_{a2})
MOPS	7.20	Borate	13.30 (pK_{a3})

The equilibrium theory in buffer solutions is a fundamental concept that helps explain how buffer solutions work and maintain a relatively stable pH. Buffer solutions are aqueous solutions containing a weak acid and its corresponding conjugate base (or a weak base and its corresponding conjugate acid) that are able to resist the pH shift that would otherwise be caused by a substantial addition of a strong acid or base. The equilibrium theory in buffer solutions is based on the principles of chemical equilibrium, so, in a buffer solution, a weak acid (HA) and its corresponding conjugate base (A^-) are in dynamic equilibrium with each other, as the weak acid can donate protons (H^+) to the solution, forming H_3O^+ ions and the conjugate base can accept

protons (H^+), forming HA molecules ($HA \rightleftharpoons H^+ + A^-$). When an acidic substance (H^+) is added to the buffer solution, the excess H+ ions react with the conjugate base (A^-) to form more weak acid (HA), and when a basic substance (OH^-) is added, the OH^- ions react with the weak acid (HA) to form water. These reactions shift the equilibrium but do not cause significant changes in the pH of the solution because the buffer system can absorb or release protons to counteract the pH change (11).

The inclusion of multiple components buffers with different pKa values allows the buffer to cover a wide pH range effectively. This flexibility is particularly valuable in the early stages of method development, as there may not exist certainty about the exact pH conditions that will yield the best results. Therefore, multi-component buffers allow the exploration of a wider pH range, which can help identify the pH at which the method performs optimally.

As a multi-component universal buffer solution that can cover a broad pH range (typically from around pH 2 to pH 12), the Britton-Robinson buffer can be composed of a mixture of weak acids and their corresponding conjugate bases and its exact composition can be adjusted to achieve the desired pH range for a specific experiment or application. Commonly used components in Britton-Robinson buffer solutions include boric acid (H_3BO_3), acetic acid (CH_3COOH) and phosphoric acid (H_3PO_4), which can donate a proton to the solution, as well as sodium hydroxide (NaOH), a base component that helps to control and raise the pH to the desired level and that can react with the weak acids in the buffer to form their respective conjugate bases (12).

Regarding the pH of the buffer, it can modify the charge of the analyte and change the EOF, and consequently affect separation. Alterations in pH are particularly useful when solutes have accessible isoelectric point (pI) values, such as peptides and proteins. Working above and below the pI value will change the solute charge and cause the solute to migrate either before or after the EOF. Below its pI a solute possesses a net positive charge and migrates toward the cathode, ahead of the EOF. Above the pI the opposite occurs (1).

The accessible pH range can vary from below 2 to more than 12, in the fused silica capillary, but is usually limited by the pH stability of the solute (1).

It can also be added organic solvents to the aqueous buffer, such as methanol and acetonitrile, in order to increase the solubility of the solute or to affect the degree of

ionization of the sample. The addition of these organic modifiers to the buffer generally causes a decrease in the EOF (13).

Other buffer additives can be added to the buffer, such as: surfactants, to increase solubility or to act as ion pairing agents; organic amines, to change wall charges; metal ions, to reduce wall adsorption; urea, as a denaturing agent; linear polymers, to increase viscosity, mask wall charges and introduce a sieving selectivity into the system; and complexing agents, that may affect the separation by introducing very selective interactions like stereoselectivity (3–5).

1.2.5 Internal Standard

Many aspects must be considered when optimizing the quantitative performance of CE, since its injection precision performance is affected by numerous factors. During a CE injection, the volume injected is very small and it is difficult to inject such small volumes in a reproducible manner. The volume injected is directly related to the pressure difference and the time that the pressure is applied, as well as the capillary diameter and length and the viscosity of the sample solution and the buffer. This can lead to variable injection volumes and peak areas. The primary solution to improved precision is using an Internal Standard (IS) (14,15). The use of internal standards is highly recommended as it not only significantly improves the quantitative performance of capillary electrophoresis methods in terms of precision (eliminating all injection volume-related sources of error), but also linearity (1).

The main requirement for the choice of the IS is that the substance gives good peak shape and is resolved from the analytes of interest and any other peaks in the separation, while migrating reasonably near the solute peak of interest. Other requirements for an appropriate internal standard include that it is stable in solution (to prevent the formation of degradation products), cheap and readily commercially available in a high purity form, readily soluble in the diluent required, possesses acceptably high UV activity at the desired wavelength, is inexpensive and is non-toxic (14).

When the sample is analyzed, the peaks for both the internal standard and the analyte are integrated. The area of the analyte peak is divided by the area of the internal standard peak to produce a peak area ratio (PAR) value. If a higher injection volume inadvertently occurs, then the areas of both the internal standard and solute peaks will

increase to the same extent and the PAR will remain constant. Conversely, if the injection volume is smaller both peaks will be correspondingly smaller and the PAR value will remain constant (14).

Apart from the volume injected, peak areas are also related to an analyte's migration time, since it influences peak resolution, shape, detector sensitivity (the length of time that an analyte spends within the detector's detection window can affect the detector's ability to measure the analyte's signal, leading to variations in signal intensities and peak areas), signal-to-noise (S/N) ratio, and retention time variability. Therefore, poor peak area precision will be obtained if variable migration times occur throughout a sequence and in order to help with the migration time reproducibility, precautions such as capillary rinsing and elimination of buffer depletion effects are employed in routine applications. Nevertheless, during the course of each separation slight variability can occur in the level of current, solution viscosity and temperature, which can lead to slightly different migration times for the peaks for each analysis. This creates a peak area bias and to help minimize it, peak areas must be divided by the corresponding migration time to give the corrected area, in order to compensate for the shift in migration time from run to run. The resulting parameter is referred to as the Time-Corrected Area Ratio (TCAR), where the "Time-Corrected" part of TCAR takes into account any variations in migration time due to changes in experimental conditions, and the "Area Ratio" part involves comparing the peak areas of the analyte and the internal standard, correcting for variations of the injection volume (3,8).

1.3 Active Pharmaceutical Ingredient

1.3.1 Nebivolol Hydrochloride

Nebivolol Hydrochloride (NEB) is a third generation highly selective β_1 receptor-adrenergic blocker and has a unique pharmacologic profile from other drugs in its class, as it causes nitric oxide-mediated vasodilation, decreased peripheral vascular resistance, increased stroke volume, ejection fraction, and cardiac output, by stimulating endothelial nitric oxide synthase via β_3 agonism, in addition to cardioselectivity mediated by β_1 receptor blockage, which consequently leads to decreased resting heart rate, exercise heart rate, myocardial contractility, systolic blood

pressure, and diastolic blood pressure (16–18). Its chemical structure can be seen in Fig.4.

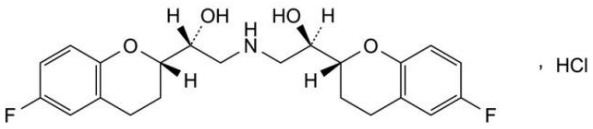

Figure 4: Chemical structure of Nebivolol Hydrochloride (19).

It is approved for the treatment of essential hypertension and of stable mild and moderate chronic heart failure. In hypertension, the recommended starting dose is 5 mg once daily and it is given orally as the hydrochloride although doses are expressed in terms of base (each 5 mg tablet of nebivolol contains 5.45 mg of nebivolol hydrochloride) (20).

NEB is a racemate of two enantiomers, d-nebivolol and l-nebivolol, with the stereochemical designations of [SRRR]-nebivolol and [RSSS]-nebivolol, respectively. Their chemical structure can be seen in Fig.5. The enantiomers have unequal potency regarding β-receptor blocking activity and nitric oxide mediated vasodilation, for instance, the d-isomer conveys the β_1-blocking effects, and the l-isomer is primarily responsible for nitric oxide stimulation (21,22).

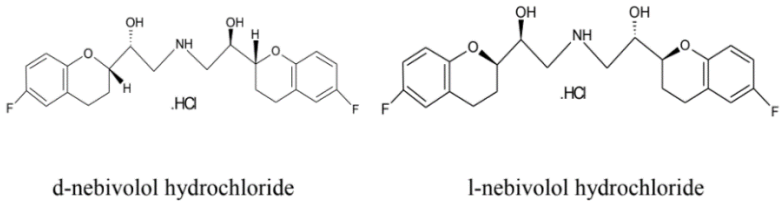

Figure 5: Chemical structure of the two NEB enantiomers (23).

Nebivolol hydrochloride is a salt, and the chemical group that becomes protonated is the amine (NH) group, which becomes NH^+ and forms an ion pair with the chloride ion (Cl^-) from the hydrochloride component. In an acidic environment, the Active Pharmaceutical Ingredient (API) is protonated and then salified. This stable salt formation is common in pharmaceuticals and is often used to improve the solubility,

stability, and other properties of the drug. In a basic environment, conversely, the corresponding free base precipitates (24). The physical and chemical properties of NEB are shown in Table 2.

Table 2: Physical and chemical properties of nebivolol hydrochloride (19,25).

Chemical Formula	$C_{22}H_{26}ClF_2NO_4$
ATC Code	C07AB12
Appearance	White or almost white crystalline powder
Molecular Weight (M_r)	441.9 g/mol
Solubility	Very slightly soluble in water (0.0403 mg/mL), sparingly soluble in methanol, very slightly soluble in heptane
Melting Point	220-222 °C
logP	2.44
logS	-4
pKa (Strongest Acidic)	13.52
pKa (Strongest Basic)	8.9
Maximum Absorbance	281 nm

Being a Biopharmaceutics Classification System class-2 drug, which has low solubility and high permeability, NEB can have poor dissolution in the gastrointestinal tract. This can lead to reduced bioavailability and formulation approaches are often needed to improve the solubility of these drugs.

1.3.2 Pharmacokinetics

Both nebivolol enantiomers are rapidly absorbed after oral administration and this absorption is not affected by food. The maximum plasma concentration is 1.42 μg/L and the time to reach the peak concentration for racemic mixture is 0.5-2 hours (23).

The oral bioavailability of nebivolol averages 12% in fast metabolizing patients and is virtually complete in slow metabolizers. It undergoes extensive metabolism in the liver

and is metabolized via alicyclic and aromatic hydroxylation, N-dealkylation and glucuronidation and, in addition, glucuronides of the hydroxy-metabolites are formed. The metabolism by aromatic hydroxylation is subject to the CYP2D6 dependent genetic oxidative polymorphism. Poor metabolizers may require lower doses. The pharmacokinetics of nebivolol are not affected by age. Plasma concentrations are dose-proportional between 1 and 30 mg (20,23).

In plasma, both nebivolol enantiomers are predominantly bound to albumin. Plasma protein binding is 98.1% for SRRR-nebivolol and 97.9% for RSSS-nebivolol, with limited distribution in adipose tissue due to its lipophilicity and hence no need for dosage adjustment in obese patients. The volume of distribution is 695 to 2755 liters (23).

The elimination half-life of nebivolol is about 10 hours, increased by 5 times in poor metabolizers, and for its metabolites it is about 24 hours. One week after administration, 38% of the dose is excreted in the urine and 48% in the feces. Urinary excretion of unchanged nebivolol is less than 0.5% of the dose (23).

1.4 Excipient

In order to increase weight and improve content uniformity (acting as a filler) of the ODT, the excipient Isomalt, more specifically, the grade GalenIQ™ 721, was used as a diluent in the formulation.

Isomalt is a mixture of two stereoisomers: 6-O-a-D-glucopyranosyl-D-sorbitol (1,6-GPS) and 1-O-a-D-glucopyranosyl-D-mannitol dihydrate (1,1-GPM). Their chemical structure can be seen in Fig.6, and their chemical formula is, for 1,6-GPS, $C_{12}H_{24}O_{11}$ (M_r: 344.32 g/mol) and for 1,1-GPM, $C_{12}H_{24}O_{11} \cdot 2\ H_2O$ (M_r: 380.32 g/mol). 1,6-GPS crystallizes without water and is more soluble than 1,1-GPM. By shifting the ratio of the two components, the solubility and crystal water content can be adjusted (26,27).

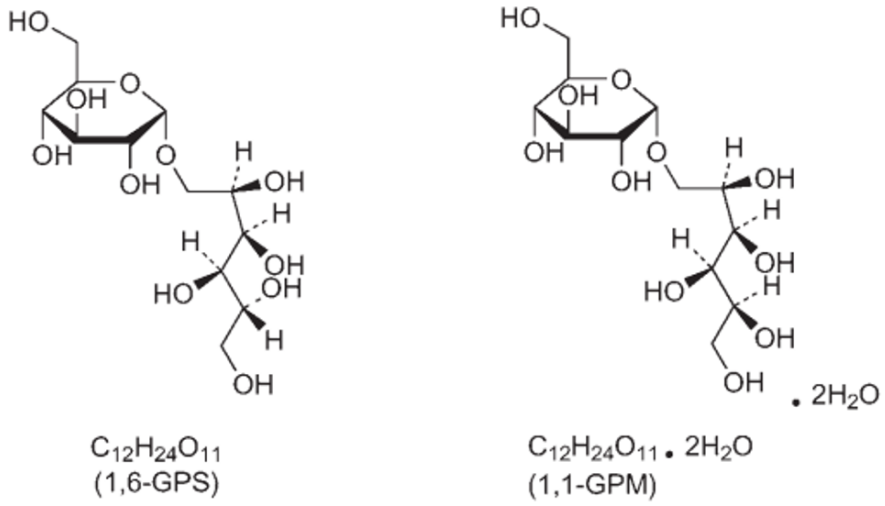

Figure 6: Chemical structure of the two isomalt stereoisomers (27).

Isomalt is a non-cariogenic excipient used in a variety of pharmaceutical preparations including tablets or capsules, coatings, sachets, and suspensions, and in effervescent tablets. It can also be used in direct compression and wet granulation (being GalenIQ 721 used in direct compression). It can act as a coating agent, granulation aid, medicated confectionary base, sweetening agent and tablet and capsule diluent (28). It is a sugar alcohol (polyol) that occurs as a white to almost white powder, granular or crystalline substance. It has a pleasant sugar like taste with a mild sweetness approximately 50–60% of that of sucrose. Additionally, it exhibits considerable resistance to acids and microbial influences and has no reducing groups, so it does not react with other ingredients in a formulation, for example, with amines in Maillard reactions (26,27).

GalenIQ 721 is an agglomerated spherical isomalt with a GPM:GPS ratio of 1:3, whose preferred application is in slow to very fast disintegrating tablets. It presents several benefits, namely: high agglomerate stability and excellent flow; its morphology ensures homogeneity of the mix and content uniformity; very low compression forces required; filler and binder function (additional binders in general not required) (26,27).

Regarding its properties, it has a solubility of 42 g/100 g solution at 20°C water, its bulk density is 0,42 g/cm³ and it is very low hygroscopic. It is freely soluble in water, but practically insoluble in ethanol (27,28).

1.5 Method Development

1.5.1 Analytical Target Profile

An Analytical Target Profile (ATP) defines the intended purpose of the Analytical Procedure and consists of its description, as well as the description of the appropriate details on the product attributes to be measured and relevant performance characteristics with associated performance criteria. The ATP outlines the performance requirements for a single attribute or a set of quality attributes (29).

1.5.2 Knowledge Management

Knowledge management is of paramount importance in analytical procedure development. Prior knowledge, whether explicitly or implicitly used, serves as a foundation for making informed decisions and encompasses both internal sources, derived from a company's own proprietary development and analytical expertise, as well as external sources (29).

1.5.3 Risk Management

The use of quality risk management is encouraged to aid in the development of a robust analytical procedure to reduce the risk of poor performance. Risk assessment is typically performed early in analytical procedure development and is repeated as more information becomes available. Risk assessment can be formal or informal and can be supported by prior knowledge (29). One of the simplest techniques that are commonly used to structure risk management by organizing data and facilitating decision-making is a cause and effect diagram (Ishikawa diagram) (30). Using this tool, Fig. 7 represents analytical procedure parameters identified (factors and operational steps) with potential impact on the CE performance.

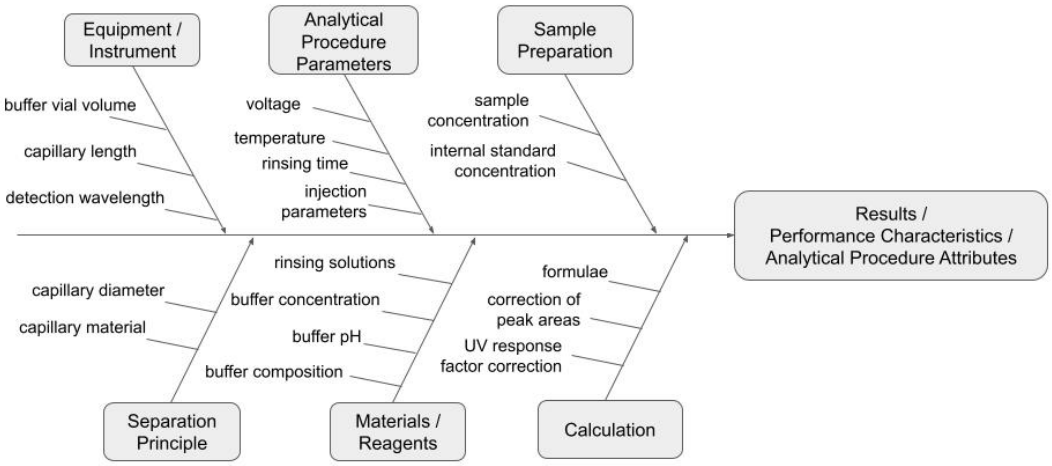

Figure 7: Parameters with potential impact on the performance of the procedure.

1.5.4 Optimisation

1.5.4.1 Experimental Design

According to International Council for Harmonisation of Technical Requirements for Pharmaceuticals for Human Use (ICH) Q8 guidelines (31), Quality by Design (QbD) is “A systematic approach to development that begins with predefined objectives and emphasizes product and process understanding and process control, based on sound science and quality risk management.”.

An important aspect of QbD is to know how process and formulation parameters could affect the product characteristics and subsequent optimization of these parameters should be known in order to monitor these parameters online in the production process. Similarly, when we apply QbD principles to analytical methods (referred to as Analytical QbD or AQbD), the objective is to develop a method that is well-understood, tailored to its specific purpose, and robust enough to consistently deliver the intended performance over its entire lifespan. The extensive knowledge acquired in the AQbD process is utilized to define a Method Operable Design Region (MODR). The MODR represents a multidimensional parameter space defined by the method's factors and settings, which provides suitable method performance (31,32).

Experimental design plays a pivotal role in AQbD by providing a structured and systematic approach to method development and optimization. Experimental design is employed in method development to systematically investigate the influence of various factors on the analytical method's performance and involves all aspects of planning and conducting experiments, including the selection of factors, levels, the sequence of runs, randomization, replication, and data collection. Within experimental design, Design of Experiments (DoE) is a specific methodology and structured approach, primarily focused on optimizing experiments and achieving efficient results. Prior knowledge and risk assessment play a crucial role in selecting the parameters to investigate. Once the most critical factors that affect the method's outcome are identified, common designs like full factorial, fractional factorial, and response surface designs, are used to optimize the method. These statistical experimental designs help determine the optimal levels of each factor to achieve the desired analytical performance, such as accuracy, precision, and robustness (33).

Opposed to full factorial designs, that are used to explore all factor combinations comprehensively, fractional factorial designs are employed when it is needed to reduce the number of experimental runs but still obtain valuable insights into factor effects and interactions. On the other hand, response surface designs are suitable for optimizing a process or system by efficiently exploring the factor space around an optimal point, so it requires knowledge of the approximate location of the optimum.

Response Surface Methodology (RSM) consists of a set of mathematical and statistical methods developed for modelling phenomena and finding combinations of a number of experimental factors (variables) that will lead to optimum responses. With RSM, several variables are tested simultaneously with a minimum number of trials, according to special experimental designs, which enables to find interactions between variables. In addition, RSM has the advantage of being less expensive and time-consuming than the classical methods. Among the best-known response surface methodologies are Box-Behnken Design, Central Composite Design, and Doehlert Design (34).

Central Composite Design (CCD) combines factorial points (which represent combinations of factor levels at both their high (+1) and low (-1) settings and help identify main effects and interactions between factors), center points (which are experiments conducted at the midpoint of the factor ranges and provide an estimate of the experimental error or noise, and help determine if the response surface is linear or

exhibits curvature) and axial points (that extend outward from the center of the factor space along each factor direction, allowing for the exploration of curvature in the response surface and provide information about quadratic terms in the model (35).

A Face-Centered Central Composite Design is a valuable variation of CCD that is particularly useful to focus on exploring the behavior of factors at their high and low extremes while maintaining the key properties of a CCD (33). This design locates the axial points on the centers of the faces of the cube, as illustrated in Fig.8.

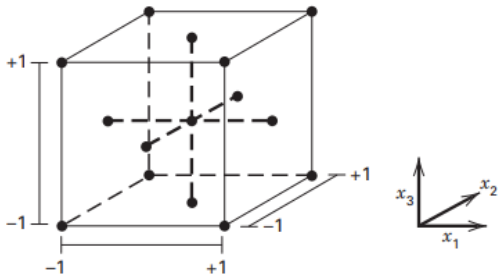

Figure 8: A face-centered central composite design for k=3, where k=number of different factors incorporated in the study (33).

1.5.4.2 Robustness

The robustness of an analytical procedure is a critical measure of its ability to consistently meet the expected performance requirements. In essence, it assesses the method's reliability under varying conditions, and it is evaluated through deliberate variations in the parameters of the analytical procedure. These variations are introduced to determine how well the method can withstand changes in conditions that might occur during routine use. Thereby, this evaluation helps establish confidence in the method's reliability, consistently producing accurate and precise results, even in the face of parameter variations (29).

For most procedures, robustness evaluation is conducted during development. If the evaluation of robustness was already conducted during development, it does not need to be repeated during validation (36).

Various methodologies, both classical and multivariate, can be employed to evaluate robustness. These include the one-factor-at-the-time approach and factorial design. The Plackett-Burman Design (PBD), a two-level fractional factorial screening design, can

be employed to assess the robustness of the optimized process. PBD's primary purpose is to screen and identify influential factors efficiently, making it a useful choice at various stages of experimental design and process optimization, either as a screening tool before detailed experimentation or as a tool for refinement and robustness testing after an initial RSM study, as it can be used when merely the key factors are concerned (37).

1.6 Method Validation

Validation is the confirmation by examination and provision of objective evidence that the particular requirements for a specified intended use are fulfilled. Furthermore, the purpose of validation of an analytical procedure is to establish the effectiveness of the analytical method with a high degree of accuracy, through experimental tests (36).

Typical performance characteristics and related validation tests for measured product attributes can be seen in Fig. 9.

Type of measured product attribute / Analytical Procedure Performance Characteristics to be demonstrated (2)	IDENTITY	IMPURITY (PURITY) Other quantitative measurements (1)		ASSAY content/potency Other quantitative measurements (1)
		Quantitative	Limit	
Specificity (3)				
Specificity Test	+	+	+	+
Working Range				
Suitability of Calibration model	-	+	-	+
Lower Range Limit verification	-	QL (DL)	DL	-
Accuracy (4)				
Accuracy Test	-	+	-	+
Precision (4)				
Repeatability Test	-	+	-	+
Intermediate Precision Test	-	+ (5)	-	+ (5)

Figure 9: Typical performance characteristics and related validation tests for measured product attributes (36).

1.6.1.1 Specificity / Selectivity

This characteristic is described as the ability to discriminate unequivocally the analyte in the presence of potential interfering substances that are expected to be present, such

as excipients and impurities, confirming that the signal measured is caused solely by the analyte (36).

For an assay method, specificity is assessed by verifying the absence of interfering peaks at the analyte retention time when spiking a sample with appropriate levels of impurities, such as degradation products and synthesis intermediates, in addition to excipients from the formulation at their expected level as well as the internal standard solution (36).

It is also important in CE to assess the repeatability of selectivity by repeatedly injecting and analyzing standard and test solutions with the same vial. This is necessary as electrolysis of the buffer can occur under the applied voltage, which yields a change in the electrolyte pH and may alter the EOF velocity and the API ionization (38).

1.6.1.2 Working Range

The reportable range of an analytical procedure is the interval between the lowest and highest results that maintain suitable levels of precision, accuracy, and response. Depending on the sample preparation (for example, dilutions) and the analytical procedure selected, the reportable range will lead to a specific working range (36).

The working range is the concentration range in which the analytical procedure provides meaningful results. There may be two working ranges: one before sample preparation (sample working range) and one when the sample is presented to the analytical instrument (instrument working range).

The range of an analytical method is established through linearity studies, and it encompasses the upper to the lower concentration of the analyte in the sample, in which the linearity test was successfully conducted. Therefore, a linear relationship between analyte concentration and response should be evaluated across the working range of the analytical procedure to confirm the suitability of the procedure for the intended use. For the establishment of linearity, a minimum of five concentrations appropriately distributed across the range is recommended, however, additional concentrations may be required for more complex models. The ICH guideline Q2(R2) on validation of analytical procedures recommends specific criteria for the low and high ends of the reportable range for assay tests, where the low end should be 80% of the declared

content or 80% of the lower specification limit and the high end should be 120% of the declared content or 120% of the upper specification limit (36).

Regarding the validation of lower range limits, the limit of detection (LOD) and the limit of quantification (LOQ) can be estimated using different approaches, including the determination of the S/N ratio, calculating the standard-deviation/slope ratio and by visual evaluation. Samples with known analytical concentration are prepared and the lowest concentration at which the analyte can be reliably detected, but not necessarily quantitated (LOD) is established, as well as the minimum level at which the analyte can be quantified with an acceptable level of precision and accuracy (LOQ). It is generally accepted that a S/N ratio at the LOQ should be at least 10, and for the LOD, at least 3 (38,39).

1.6.1.3 Accuracy and Precision

Accuracy in analytical testing refers to how closely the test results match the true or theoretical value, and it quantifies the agreement between experimental measurements and an accepted reference value. This assessment helps evaluate the impact of systematic errors on a method.

To assess it, at least 9 determinations are made at a minimum of 3 different concentration levels within the specified range (3 replicates at 3 concentrations). Accuracy should be reported as the mean percent recovery by the assay of a known added amount of analyte in the sample or as the difference between the mean and the accepted true value along with the confidence intervals (36).

As for precision of an analytical procedure, it expresses the degree of scatter between a series of measurements under the prescribed conditions. Precision can be considered at three levels: repeatability, intermediate precision and reproducibility. Regarding repeatability, it refers to the variability when the method is performed by the same analyst on the same piece of equipment over a short timescale and it can be assessed using a minimum of 9 determinations covering the reportable range for the procedure (3 concentrations/3 replicates each). The precision of an analytical procedure is usually expressed as the variance, standard deviation or coefficient of variation of a series of measurements (36).

2 Materials And Methods

2.1 Materials

Nebivolol Hydrochloride was a gift from A. Menarini Manufacturing Logistics and Services S.r.l. (Firenze, Italy); Boric Acid (≥ 99,5%, M=61.83 g/mol) was purchased from Sigma-Aldrich Co. (St. Louis, MO, USA); Acetic Acid Glacial (100%, 17.49 M) was supplied by E. Merck (Darmstadt, Germany); Phosphoric Acid BioUltra (≥85%,14.61 M) was purchased from Sigma-Aldrich Co. (St. Louis, MO, USA); GalenIQ™721 (Isomalt Ph. Eur) was supplied by BENEO-Palatinit GmbH (Mannheim, Germany); Procaine Hydrochloride (minimum 97%) was purchased from Sigma-Aldrich Co. (St. Louis, MO, USA) and used as the internal standard; Ultrapure water from Elix® (Millipore, Burlington, MA, USA) was used.

2.2 Methods

2.2.1 Method Development

Employing the principles of AQbD, and following ICH Guidelines Q2(R2) and Q14, the development process was organized into seven pivotal stages:

1. Setting the Analytical Target Profile;
2. Knowledge Management;
3. Risk Assessment;
4. Adopting the enhanced approach of ICH Q14, using the Response Surface Methodology;
5. Establishing the Method Operable Design Region;
6. Ensuring Robustness;
7. Final Method Validation.

2.2.2 Analytical Target Profile

The ATP was determined to quantify NEB across various tablet formulations and tailored to different purposes: routine content uniformity analysis, dissolution tests, and accelerated degradation studies. The goal was to achieve baseline separation of NEB and PRO, while ensuring they remained distinct from any possible overlapping

excipient peaks, such as GalenIQ 721, all within a short analysis time frame. The criteria set for Validation Performance were:

- Selectivity: Full resolution of the analyte peaks with no overlap from tablet excipients.
- Limit of Quantification: Fixed below 0.008 mg/mL, which was the lowest theoretical concentration expected across all samples.
- Working Range: Established for the API between the LOQ and 1.2 mg/mL, accommodating up to 120% of the maximum sample concentration.
- Accuracy: Expected recovery values for NEB ranged between 98% and 102%.
- Precision: Measured by repeatability, where Relative Standard Deviation (RSD) values for the API were capped at 3%. However, at the LOQ, a slightly more lenient RSD of up to 15% was accepted.

2.2.3 Capillary Electrophoresis instrumentation and analysis

Capillary electrophoresis analysis was performed on an Agilent 7100 Capillary Electrophoresis System (G7100A Serial Number) with a UV-Vis detector, using bare fused silica capillaries from CM-Scientific Ryefield (Dublin, Ireland) with 48,5 cm of total length (40 cm of effective length) for direct polarity injection and 33 cm of total length (8,5 cm of effective length) for short-end injection, 50μm I.D. and 375 μm O.D.

Each new capillary was rinsed with 1N HCl, 0.1N HCl, 95:5 MeOH:HCl 1N, MeOH and water for 5 minutes each. Daily, the capillary was rinsed with 0.1N HCl, 95:5 MeOH:HCl 1N and water for 2 min each before use.

In order to analyze which one would give the peaks a better shape and also which would give the current more stability (due to possible irregularities in the surface), two different pre-conditioning steps performed before each injection were tested:

1. 120s NaOH 0.1M, 120s H_2O, 240s BGE;
2. 60s MeOH, 60s MeOH:HCl 1N (95:5), 60s H_2O, 60s BGE.

The samples were injected by hydrodynamic injection at 50 mbar for 5 sec, followed by a plug injection of BGE (50 mbar for 5 sec). Later in the project, it was opted to use reverse polarity mode, in a short-end analysis configuration, applying a first -50 mbar vacuum for 5 s for sample injection, then -50 mbar for 5 s for plug injection. Given the

short-end nature of the runs, the sample vial was placed at the conventional outlet end of the cassette, while an empty vial was placed at the inlet end. Owing to the standard instrumental configuration of CE, only the inlet end was subjected to active pressure control, so the negative pressures were in fact directly applied to the empty vial at the inlet end, while the sample (first interval) and the plug (second interval) were drawn in from the outlet end by the pressure difference.

Wavelength for sample detection was chosen by examining the nebivolol hydrochloride UV spectrum and considering its maximum absorbance.

The temperature was kept constant at 22°C and the capillary ends were kept levelled.

Different separation voltages were tested, starting with voltages of +25 kV and +30 kV, and in later experiments with a range of -15 kV to -25 kV, for short-end injection.

Experiments were carried out using a Britton-Robinson buffer composed of 0.5 M phosphoric acid (H_3PO_4), 0.5 M boric acid (H_3BO_3) and 0.5 M acetic acid (CH_3COOH). 25 mM BGE with pH range 2-4 were prepared by mixing the adequate volume of Britton–Robinson buffer with water, to about 80% of the final volume, adjusting pH with 1 M NaOH and 0,1 M NaOH, using a Metrohm 713 pH Meter (Herisau, Switzerland), and subsequently filling up to the volume with water. In later stages of the method development, a 15 mM-35 mM phosphoric acid buffer with pH range 2-4 was used instead, to make the BGE simpler, once the pH working range was already known, and it was enough to use only H_3PO_4.

OpenLab CDS ChemStation Edition (Agilent Technologies) was used for instrumental control, electropherogram acquisition, and data analysis.

2.2.4 Stock solutions and sample preparation

A stock solution of nebivolol hydrochloride with a final concentration of 10 mg/mL was prepared by dissolving NEB in methanol (MeOH).

A stock solution of galenIQ 721 with a final concentration of 10 mg/mL was prepared by dissolving the component in MilliQ water.

Procaine hydrochloride (PRO) was chosen as the internal standard, considering it has a high pKa and will therefore easily exist in its protonated form with the acidic pH of the buffer, as it had to be protonated in order to run in the capillary. It is stable in solution

and soluble in MeOH, while possessing acceptably high UV activity at the working wavelengths of detection. Its stock solution with a final concentration of 10 mg/mL was prepared by dissolving the component in MeOH.

All stock solutions were stored at 4°C and used within 1 week, while all the standard solutions were prepared daily, by diluting the stock solutions in a 2 mL Eppendorf tube (up to a maximum of 1.5 mL), to obtain the desired final concentrations.

Standard NEB solution with a concentration of 0.5 mg/mL was prepared by diluting the stock solution in 100% MeOH.

A GalenIQ 721 sample was tested, with a 0.5 mg/mL concentration, by diluting the proper volume of stock solution in 100% H_2O.

A sample containing both 0.5 mg/mL NEB and 0.5 mg/mL GalenIQ 721 was prepared in 95% MeOH, by adding 25 µL of NEB 10 mg/mL stock solution, 25 µL of GalenIQ 10 mg/mL stock solution and 450 µL of MeOH, for a final volume of 500 µL.

After testing these standard solutions, varying the values of parameters such as the voltage and pH buffer, and modifying the pre-conditioning performed before each injection, a sample containing 0.5 mg/mL NEB, 0.5 mg/mL galenIQ 721 and 0.5 mg/mL PRO in 95% MeOH was analysed. It was prepared by adding 25 µL of NEB 10 mg/mL stock solution, 25 µL of GalenIQ 10 mg/mL stock solution, 25 µL PRO of 10 mg/mL stock solution and 425 µL of MeOH, for a final volume of 500 µL.

2.2.5 Method Optimisation

In order to investigate the influence of different factors on the analytical method's performance, experimental design was generated, and statistical analysis of the experimental data was performed. The optimization through RSM and MODR identification using Monte Carlo Simulations, was carried out through MODDE 13 software (Sartorius Data Analytics AB, Göttingen, Germany), allowing contour plots and probability maps to be drawn.

Critical Methods Parameters (CMPs) were represented by buffer concentration (mM), buffer pH (pH) and separation voltage (Vol), while selected Critical Method Attributes (CMAs) were resolution PRO/NEB (Res), analysis time (Tim) and efficiency of the peaks of PRO (PEf) and NEB (NEf). A Face-Centered Central Composite Design was

chosen to build a predictive quadratic model and three levels were fixed for each variable (-1, 0, +1), listed in Table 3 (voltage has been entered as its absolute value). It consisted of 8 factorial points, 3 center points, and 6 axial points (as shown in Fig. 10), giving rise to a total of 17 experiments. Responses' minimum, maximum and target values are presented in Table 4.

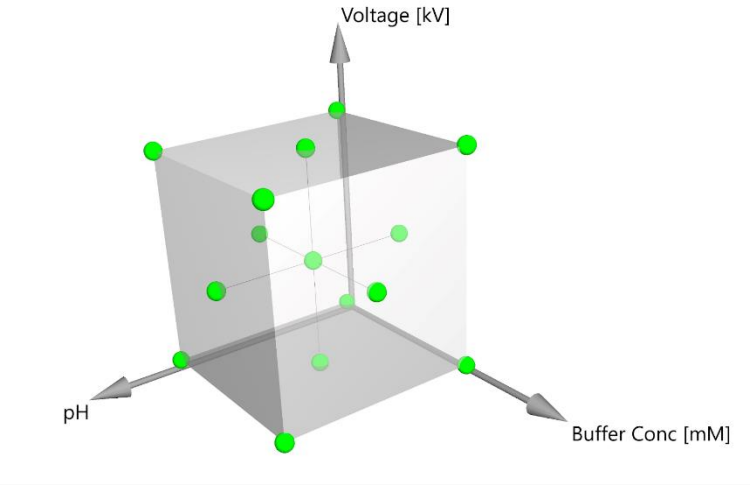

Figure 10: Design points in the experimental space.

Responses Y_1, Y_2, Y_3 and Y_4 were related to the coded variables (X_i, i = 1, 2, 3) by a full second-order polynomial, given by equation 7.

$$Y = \beta_0 + \beta_1 X_1 + \beta_2 X_2 + \beta_3 X_3 + \beta_{12} X_1 X_2 + \beta_{13} X_1 X_3 + \beta_{23} X_2 X_3 + \beta_{11} X_1^2 + \beta_{22} X_2^2 + \beta_{33} X_3^2 + \varepsilon \quad (7)$$

where Y represents the modelized CMA; X_1 (buffer pH), X_2 (buffer concentration) and X_3 (voltage) are the independent variables; β_0 is the constant term; β_1, β_2, and β_3 are the first order coefficients (linear effects); β_{11}, β_{22}, and β_{33} are the second order coefficients (quadratic effects); and β_{12}, β_{13}, and β_{23} are the interaction coefficients between X_1, X_2 and X_3; while ε is the residuals and accounts for the random fluctuations of Y that are not predicted by the model, representing the experimental error.

The samples were constituted by 0.5 mg/mL NEB, 0.5 mg/mL galenIQ 721 and 0.5 mg/mL PRO in 95% MeOH, prepared as previously mentioned. The 15 mM BGE with

pH range 2-3 were prepared by mixing 1.5 mL of 0.5 M H_3PO_4 buffer with water, to a final concentration of 50 mL, and adjusting pH as previously mentioned. The same procedure was applied to the 25 mM BGE and the 35 mM BGE, adding 2.5 mL and 3.5 mL of 0.5 M H_3PO_4 buffer, respectively.

Table 3: Variables Levels.

Variable	Unit	Levels		
		Low	Middle	High
Buffer pH	—	2	2.5	3
Buffer Concentration	mM	15	25	35
Voltage	kV	19	22	25

Table 4: Responses' minimum, maximum and target values.

Responses	Unit	Objective	Min	Target	Max
Resolution	—	Maximize	1.5	4	—
Analysis time	min	Minimize	—	1.2	3
Nebivolol Efficiency	—	Maximize	800	1300	—
Procaine Efficiency	—	Maximize	800	1300	—

The MODR was defined by creating a dense series of random launches evenly distributed throughout the experimental space, using Monte Carlo Simulations combined with the calculated models. This procedure gives a stratified probability of failure plot through the estimation of the model's confidence intervals for the true mean response.

After conducting the experimental design and even if it was demonstrated that, inside the MODR, the CMA criteria are fulfilled with a certain probability, to achieve adequate proof that the procedure maintains suitable performances during normal use, a robustness study was carried out around the optimal point, with the objective of validating it. A linear model was postulated for linking the CMPs to the CMAs, and

Plackett-Burman design, using the Nemrod-W software, was employed to estimate the coefficients. The variable levels are presented in Table 5.

Table 5: Variables Levels

Variable	Levels	
Buffer pH	2.4	2.8
Buffer Concentration	27	33
Voltage	20	22

The samples were constituted by 0.5 mg/mL NEB, 0.5 mg/mL galenIQ 721 and 0.5 mg/mL PRO in 95% MeOH, prepared as previously mentioned. The BGEs were prepared by mixing the proper volume of 0.5 M H_3PO_4 buffer with water, to a final concentration of 50 mL, and adjusting pH as previously mentioned. The pre-conditioning performed before each injection was: 120s MeOH, 120s MeOH:HCl 1N (95:5), 60s H_2O, 120s BGE.

2.2.6 Method Validation

Validation was performed according to ICH Q2(R2). The measured Product Attribute was Assay Content for the API.

Selectivity was evaluated through the observation of full resolution of the analyte peaks with no overlap from the ODT excipient, GalenIQ 721.

Linearity was evaluated using eight different concentrations of NEB, beginning from the LOQ to a 120% (1.2 mg/mL) of the highest concentration of raw sample that would be produced in subsequent phases of the project (1.0 mg/mL): 0,0005 mg/mL; 0,001 mg/mL; 0,01 mg/mL; 0,1 mg/mL; 0,5 mg/mL; 0,75 mg/mL; 1 mg/mL; 1.2 mg/mL. Each solution was injected three times, using short-end injection with a voltage of -21 kV. The buffer used was pH 2.6 30 mM H_3PO_4 and the pre-conditioning performed before each injection was: 120s MeOH, 120s MeOH:HCl 1N (95:5), 60s H_2O, 120s BGE. Calibration curves were obtained by plotting the concentration of NEB vs. the

Time-Corrected Area Ratio, calculated by equation 8, and the regression equation was established.

$$\frac{(\text{Sample Area} \div \text{Sample Migration Time})}{(\text{IS Area} \div \text{IS Migration Time})} \quad (8)$$

Accuracy was evaluated by quantifying a NEB sample of known purity and the measured vs. the theoretically expected concentrations were evaluated. This parameter was assessed using the calibration line by performing four measurements covering the working range, with four replicates each and was measured as percentage recovery, calculated by equation 9, with the confidence interval. The four points inside the calibration range included the LOQ, a low, a middle, and a high point (0.05 mg/mL; 0.6 mg/mL; 1.1 mg/mL). The same samples were also used to evaluate Precision in terms of Repeatability.

$$Recovery = \frac{\text{Theoretical Value}}{\text{True Value}} \times 100 \quad (9)$$

The confidence interval was calculated by equation 10, where *m* is the average of the recovery values, *t* is the t-value for the desired confidence level and degrees of freedom, *SD* is the standard deviation and *n* is the number of replicates (*n*=4).

$$m \pm (t \times (SD \div \sqrt{n})) \quad (10)$$

RSD was calculated by applying equation 11.

$$RSD = \frac{SD}{Mean} \times 100 \quad (11)$$

LOD and LOQ were estimated based on their signal-to-noise ratios, 3:1 and 10:1, respectively, using successive dilutions.

3 Results and Discussion

3.1.1 Knowledge Management

Knowledge Management was undertaken by running preliminary scouting experiments, aimed at the selection of a proper separation system including a proper operative mode and buffer. Scouting encompassed the selection of a suitable starting point for separation buffer millimolarity and pH, and proper capillary length and separation setup.

Although 281 nm is the maximum absorbance according to literature, sample detection was carried out at 194 nm, as it was the biggest absorbance observed in the nebivolol hydrochloride UV spectrum, shown in Fig. 11.

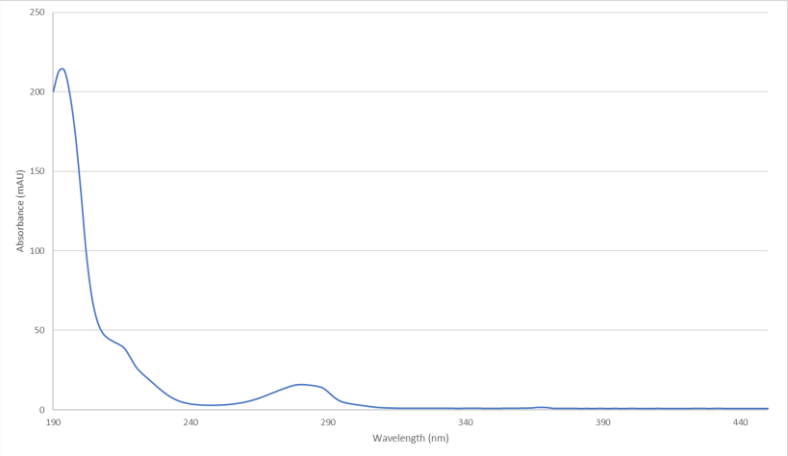

Figure 11: Nebivolol hydrochloride UV spectrum.

In order to have wider buffered zones availability from the same buffer solution, a Britton-Robinson buffer was used. The aim was to keep NEB protonated (hence under strongly acidic conditions) to be able to quantitate it using a simple buffer, without any surfactant or organic modifications. This choice originated from the consideration that using surfactants and organic modifiers tends to compromise the ability of the CE replenishment system to work, thus hindering the feasibility of simple batch analysis programming in the instrument. Moreover, simple buffer solutions tend to be more durable, both in terms of stock-time and in resistance to electrode-induced degradation during analysis.

Bare-fused silica capillaries were used, and 48.5 – 40 cm (total – effective) lengths were first employed, under direct polarity. The results were unsatisfactory, with wide peaks, long analysis times, and low reproducibility spanning scouted pH's from 2 to 4, as presented in Fig. 12, 13 and 14.

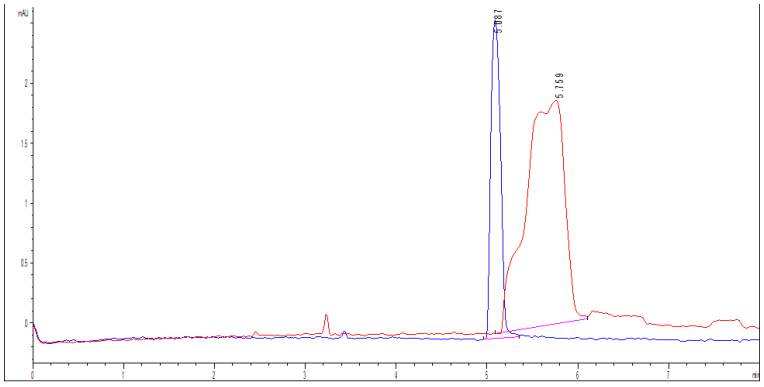

Figure 12: Two different measurements of 0.5 mg/mL NEB in 100% MeOH (BGE: $H_3PO_4/H_3BO_3/CH_3COOH$ 25mM pH 4.0; Voltage: 25 kV; Pre-cond.: 120s NaOH 0.1M, 120s Water, 240s BGE).

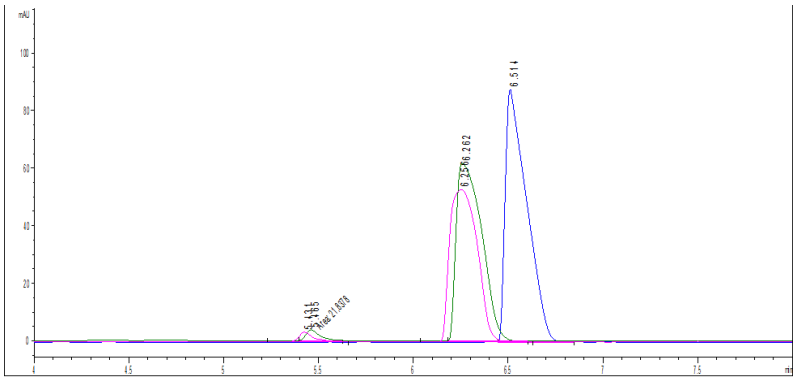

Figure 13: Three different measurements of 0.5 mg/mL NEB in 100% MeOH (BGE: $H_3PO_4/H_3BO_3/CH_3COOH$ 25mM pH 3.0; Voltage: 25 kV; Pre-cond.: 120s NaOH 0.1M, 120s Water, 240s BGE).

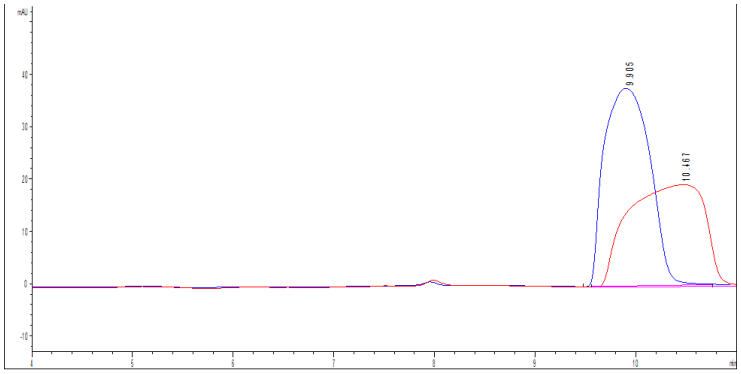

Figure 14: Two different measurements of 0.5 mg/mL NEB in 100% MeOH (BGE: $H_3PO_4/H_3BO_3/CH_3COOH$ 25mM pH 2.0; Voltage: 30 kV; Pre-cond.: 120s NaOH 0.1M, 120s Water, 240s BGE).

No interfering peaks from excipient GalenIQ 721 were found under all the scouted conditions, as it wasn't detected in any run performed, both with NEB, and GalenIQ alone, as shown in Fig.15, owing probably to its neutrality in the buffer solution and low solubility in the sample solution solvent mixture (MeOH:water 95:5). The 5% MilliQ water percentage was added to be able to simply add a 0.5mg/mL GalenIQ concentration in the injectable sample solution to test for non-interference.

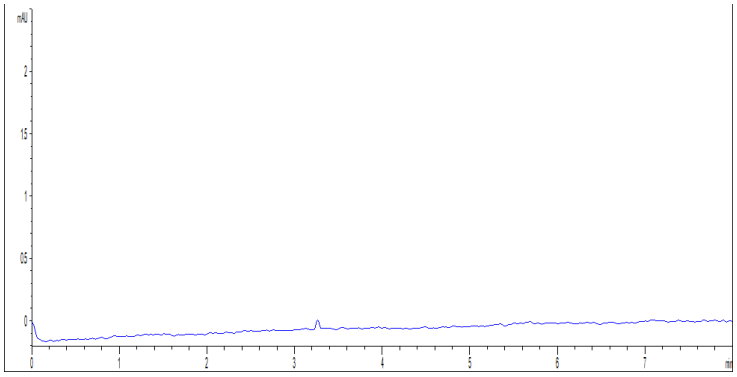

Figure 15: 0.5 mg/mL GalenIQ in 100% water (BGE: $H_3PO_4/H_3BO_3/CH_3COOH$ 25mM pH 4.0; Voltage: 25 kV; Pre-cond.: 120s NaOH 0.1M, 120s Water, 240s BGE).

33 – 8.5 cm (total – effective) lengths, using short-end injection were thus investigated, in order to contain peak diffusion exploiting lower migration lengths and times. While migration times were in fact effectively contained (3 min with respect to 10 min), reproducibility issues remained, as it can be observed in Fig.16.

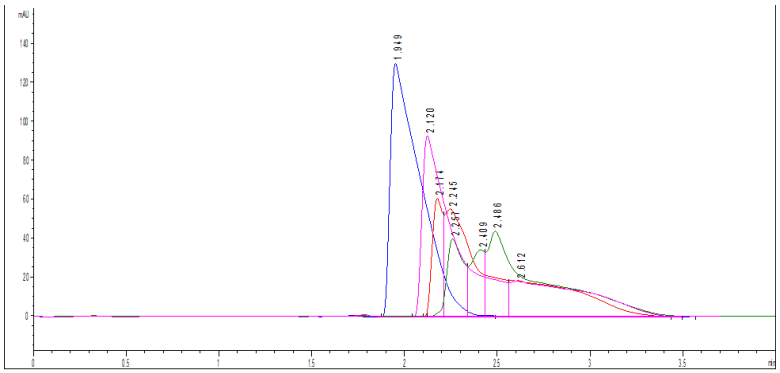

Figure 16: Four different measurements of 0.5 mg/mL NEB in 100% MeOH (BGE: $H_3PO_4/H_3BO_3/CH_3COOH$ 25mM pH 2.0; Voltage: -30kV [Short-End]; Pre-cond.: 120s NaOH 0.1M, 120s Water, 240s BGE).

These reproducibility issues were tackled by changing the pre-conditioning injection routine to: 60s MeOH, 60s MeOH:HCl 1N (95:5), 60s H_2O, 60s BGE. As capillary surface hysteresis is an established and observed effect on bare-fused silica, especially when separation pH's and conditioning solutions pH's are very different (one is strongly acidic, the other is strongly basic); it was observed how shifting from a “classic” wash cycle for bare-fused silica (NaOH and water) to an acidic one (MeOH:HCl, water), induced stabilization of both peak widths and migration times.

The best results were obtained for a 30mM pH 2 Britton-Robinson buffer, using short-end injection and acidic pre-conditioning, at 22°C and -30 kV separation voltage.

Additionally, the choice of the internal standard, procaine hydrochloride, was performed and it was observed to have good peak shape and being resolved from NEB, migrating reasonably near its peak, as presented in Fig. 17.

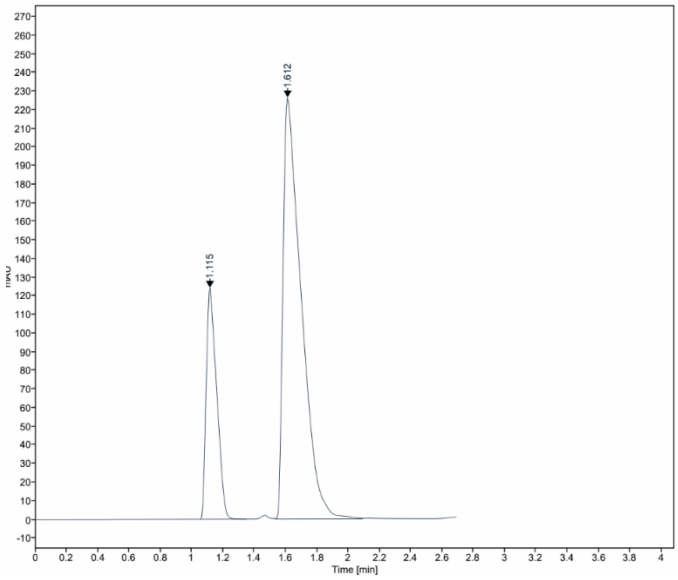

Figure 17: Electropherogram showing Procaine (IS) and Nebivolol peaks, respectively.

3.1.2 Risk Assessment and Critical Method Parameters

After defining the fundamental separation system, risk assessment was carried out to establish the risk factors and define the CMPs, whose variation was expected to exert a significant influence on method performances. From the scouting information, it was possible to fix injection-related parameters, capillary, as well as temperature and type of buffer, selected as just phosphoric acid (H_3PO_4), given the strongly acidic pH indications from the scouting and the possibility to generate lower currents (and lower joule heating) with lower amounts of charged particles in solution, along with faster migration times. On the other hand, CMPs, for which a more detailed study by DoE was needed, were selected as: separation voltage, concentration of phosphate buffer, and buffer pH.

3.1.3 Method Optimisation

3.1.3.1 Response Surface Methodology

To estimate the coefficients of the model presented in equation 7 (2.2.5 – Method Optimisation), a face-centered central composite design was planned. The experimental plan with the obtained responses is shown in Table 6.

Table 6: Face-centered central composite design matrix for the RSM procedure.

Experiment Number	Run Order	Factors				Responses		
		pH	mM	Vol	Res	Tim	NEf	PEf
1	11	2	15	19	2.72	1.728	380	386
2	16	3	15	19	2.10	1.911	571	599
3	4	2	35	19	4.05	1.745	911	1090
4	7	3	35	19	2.88	2.206	958	1118
5	14	2	15	25	2.35	1.338	237	262
6	10	3	15	25	1.95	1.476	638	520
7	5	2	35	25	3.44	1.244	692	820
8	2	3	35	25	2.74	1.554	794	914
9	3	2	25	22	3.17	1.478	508	584
10	8	3	25	22	2.67	1.668	907	916
11	13	2.5	15	22	2.20	1.500	551	681
12	6	2.5	35	22	3.39	1.615	1331	1506
13	12	2.5	25	19	3.70	1.911	1555	1588
14	15	2.5	25	25	2.95	1.356	951	1170
15	1	2.5	25	22	2.90	1.612	914	1182
16	9	2.5	25	22	3.49	1.582	1424	1454
17	17	2.5	25	22	3.01	1.588	1015	1260

It can be seen how in all experiments, resolution between PRO and NEB was more than satisfactorily reached. Furthermore, peak efficiencies were always adequate to define good peak shapes, and migration times under two minutes were found for most experimental conditions.

The quality parameters of the models were good for all the responses, ranging from 0.9371 to 0.9965 for R^2 and from 0.7642 to 0.9833 for Q^2. Hence, it was possible to employ these models for optimization, drawing graphic analysis of effects and contour plots. A graphical analysis of effects is reported in Fig. 18.

Figure 18: Graphic analysis of effects for all the CMAs.

Analyzing the graphs allowed for the acquisition of data regarding both the weight and the sign of the coefficients of the CMA models; the longer the bar, the higher the weight of the effect, with the error bars representing the confidence interval. It could be highlighted that:

- the first-order coefficient for buffer concentration was significant over all the CMAs, and was one of the pivotal effects for all, with the exception of analysis time, where its influence was overshadowed by other coefficients;
- first-order coefficients for pH and voltage were significant on most CMAs, except for NEB efficiency. Markedly, pH and voltage first-order contributions were pivotal on analysis time, with opposite signs, meaning that a higher pH would have extended analysis time, while a higher (absolute value) voltage would have shortened it;
- second-order coefficients for pH were found to be crucial in shaping both NEB and PRO efficiencies with negative contributions to both CMAs. Second-order coefficients account for the influence on the system given by the variation of the pertinent CMP at a fixed level of said CMP. This in turn means that while the first-order effect of pH may seem low or irrelevant (albeit positive), the second-order effect gives a clear indication that raising pH levels from any point

in the experimental space will give highly detrimental results for both efficiencies;

- interaction coefficients seem to exhibit low or limited influence on all the modeled CMAs.

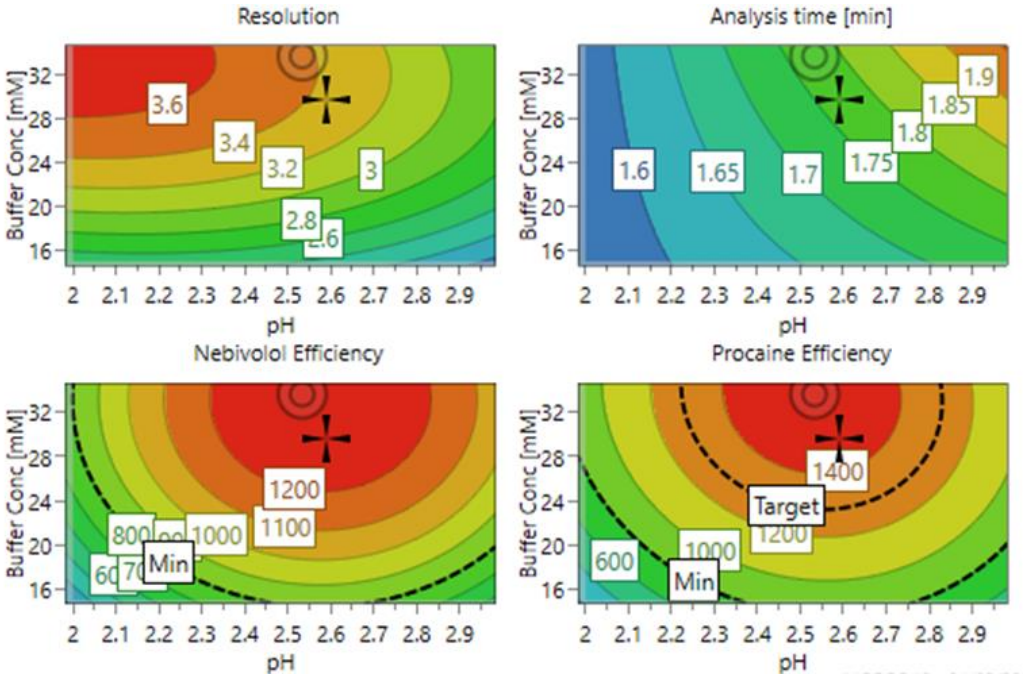

Figure 19: Contour plots showing isoresponse curves for the CMAs at the fixed value of 21 kV.

Contour plots, represented in Fig. 19, show the desired target and minimum values, when set and encompassed by the experimental system (for uniformity of representation, all four CMAs are plotted at the fixed absolute value of -21 kV).

The cross and dot show the robust and optimal setpoints, respectively. A more substantial understanding of the overall influence caused by all the coefficients can be gained by reviewing the contour plots. Resolution tends to get higher towards the far-left corner of the plot, however it is more than acceptable over all the experimental space, so its influence is minor when determining the optimal area. This means that more strain can be put on the model towards striking a balance between low analysis time and good efficiencies without running the risk of hampering resolution to the point

of analytical ineffectiveness. Since the constrained minimums and maximums were met across most of the experimental space, it is not surprising to see a sweet spot plot and a desirability plot like the ones in Fig. 20, highlighting a wide “optimal” area.

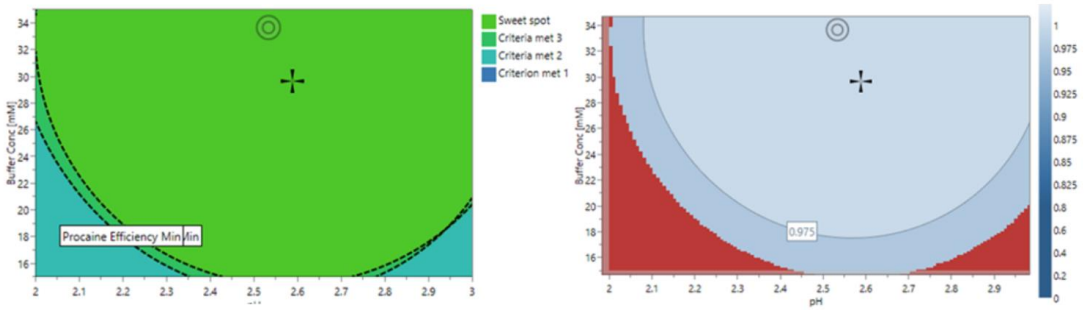

Figure 20: Sweet spot plot and desirability plot.

3.1.3.2 Method Operable Design Region

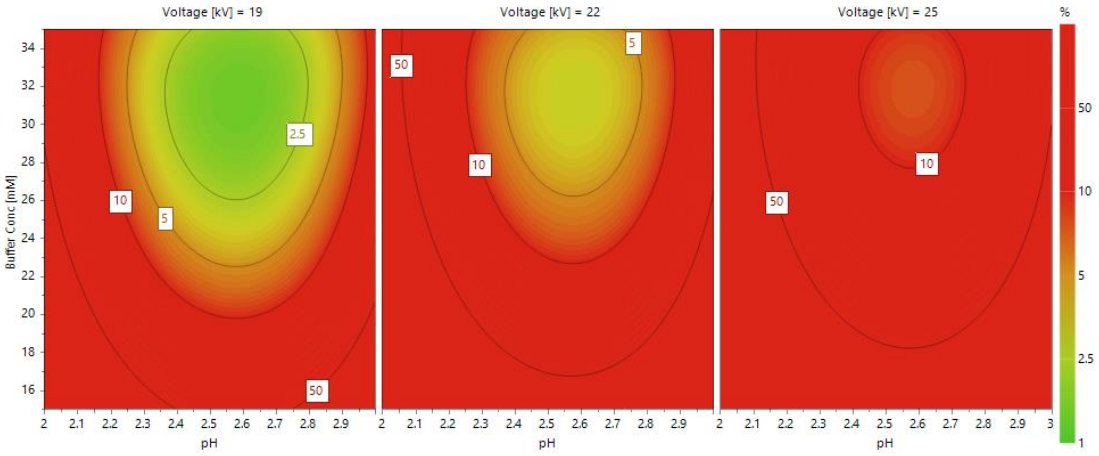

Figure 21: Probability maps highlighting the MODR for the CMAs.

The zone where the probability of fulfilling all the CMA requirements reaches a value ≥95% (desired values contained within the 5% risk of failure boundary), is reported in Fig. 21. If these maps are compared with the plots in Fig. 19, it becomes evident that incorporating the model error in the predictions of the response distributions results in a significant change of the situation. The strain imposed on the model, by maximizing resolution and efficiencies, while minimizing analysis time, without crossing the

boundaries already in place, led to the creation of a considerably narrower and defined optimal zone, much more strictly constrained by the areas of maximum efficiency.

The hypercube defining the CMAs intervals corresponding to the MODR was determined as follows: pH 2.4 – 2.7, buffer concentration 27–35mM, voltage -19 – -22kV. The working point to be used for laboratory analysis was slightly adjusted from the mathematical robust set point, in order to fix simpler values to be set for the CMPs and corresponded to: phosphate buffer 30mM, pH 2.6, separation voltage -21kV. When applying these conditions, the analysis time was lower than 2 min and the generated current was about 25 μA. The typical electropherogram is shown in Fig. 21, along with the full working point conditions, shown in Table 7.

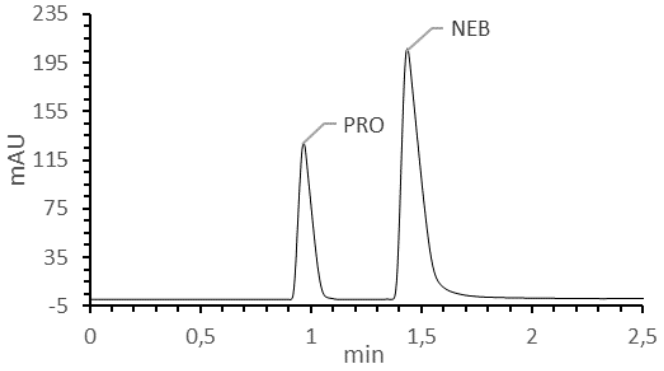

Figure 22: Typical electropherogram obtained after the analytical procedure.

Table 7: Optimized working conditions.

Working Point	
BGE	H_3PO_4 30mM pH 2.60
Capillary	33.0cm 50μm I.D. - effective length 8.5cm
Voltage	-21kV
Temperature	22°C
Injection	[Short-End] -50mbar x 5s + BGE -50mbar x 5s

3.1.3.3 Robustness

The experimental plan with the measured responses for the robustness study is shown in Table 8.

Table 8: Robustness Matrix.

Experiment Number	Factors			Responses			
	pH	mM	Vol	Res	Tim	NEf	PEf
1	2.8	33	20	3.24	1.780	1160	1108
2	2.4	33	22	3.30	1.690	1268	1283
3	2.8	27	22	2.98	1.702	1064	1148
4	2.4	27	20	3.01	1.740	951	1250

A graphic analysis of the effects is shown in Fig. 23, where the blue lines in the graphs under each response are below the statistical significance boundary.

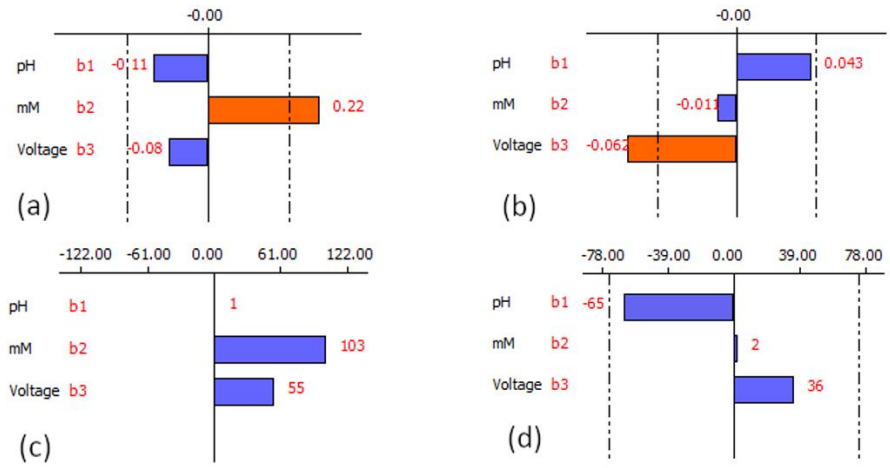

Figure 23: Graphic analysis of effects for robustness testing. Plots pertaining to: Resolution (a), Analysis time (b), NEB efficiency (c), PRO efficiency (d).

No CMP had a notable impact on NEB and PRO efficiencies, although buffer millimolarity showed an influence on resolution. Voltage, on the other hand, significantly influenced the analysis time. However, such an effect is usually observed

in an interval of 2kV (±1kV), which was the narrower range that could be selected for robustness testing due to technical constraints. The conclusion of this study indicated that particular attention should be paid to the proper control of concentration when preparing the buffer solution for the BGE.

3.1.4 Method Validation

Selectivity was demonstrated by the absence of interference with respect to the analyte and I.S. peaks. The quantification of the compounds was not impacted by the presence of other components in the matrix in any of the different sample solutions, and the peaks were well separated.

The calibration curve obtained is presented in Fig. 23.

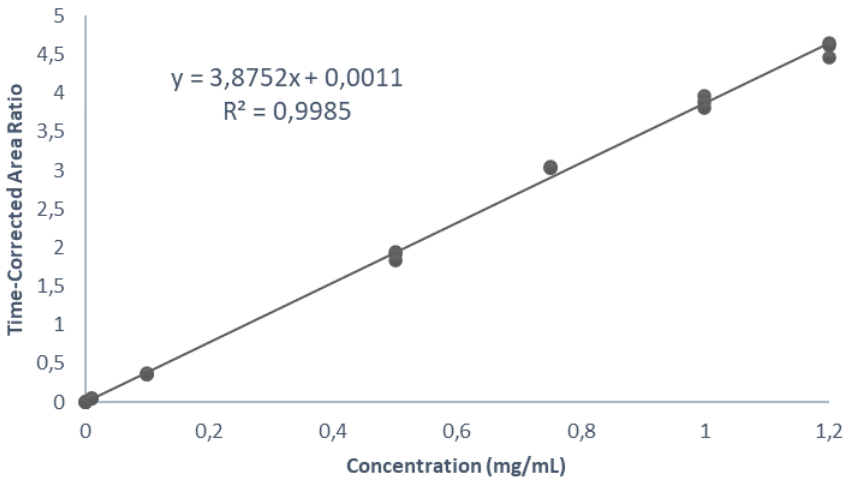

Figure 24: Calibration curve.

Linearity data, including coefficient of determination R^2, intercept, and slope of the linear regression, including their standard deviation and standard deviation of the residuals, are shown in Table 9. In the same table, data for Accuracy, Precision and determination of LOQ and LOQ can also be found.

Table 9: Full validation data.

LOD (mg/mL)	0.0003
LOQ (mg/mL)	0.0005
Working Range (mg/mL)	0.0005-1.2000
Slope a	3.8752
Intercept b	0.0011
s_a	0.0316
s_b	0.0202
$s_{x/y}$	0.1107
R_2	0.9985
Accuracy and Precision	
Concentration level (mg/mL)	0.0005
Recovery	103.4±11.8%
RSD	7.9%
Concentration level (mg/mL)	0.05
Recovery	101.8±2.7%
RSD	1.8%
Concentration level (mg/mL)	0.6
Recovery	101.3±2.9%
RSD	1.9%
Concentration level (mg/mL)	1.2
Recovery	100.4±2.1%
RSD	1.4%

Where s_a = standard deviation of the slope; s_b = standard deviation of the intercept; $s_{x/y}$ = standard deviation of the residuals; R_2 = coefficient of determination.

4 Conclusion

In this project, a capillary electrophoresis method for quantification of orally disintegrating tablets of nebivolol hydrochloride was developed, by leveraging the AQbD methodology and paving the way for alignment with the latest guidelines in the pharmaceutical analytical domain, notably ICH Q14 and Q2(R2). With the ATP clearly outlined, Knowledge Management was employed to make informed decisions regarding the CE operation mode. The selected mode was CZE, using a straightforward buffer. This buffer selection simplified the automated batch analysis of the samples, eliminating the need for surfactants or organic additives that could shorten the lifespan of the BGE and disrupt the CE replenishment mechanism. This, in turn, improved the analytical throughput and reduced the workload of the operator. Procaine hydrochloride was chosen as the internal standard considering its stability in solution and solubilization in MeOH, while possessing acceptably high UV activity at the working wavelengths of detection and having good peak shape and being resolved from NEB, migrating reasonably near its peak. The influence of CE parameters, including variations in the buffer (pH and concentration), separation voltage and preconditioning steps, were investigated, and therefore, through the AQbD approach, potential risk factors that could culminate in AP inadequacy were pinpointed, and a comprehensive grasp of the CMPs' impact on the method's efficiency was attained. RSM using Face Centered Central Composite Design and Monte Carlo Simulations was instrumental in determining the MODR. Even though the MODR itself can be considered as a robust region for the AP, within a specified probability, subsequent robustness tests further emphasized the need for precise control over concentrations of the ionic species during BGE preparation. Further application of the analytical procedure should be performed, in order to prove its successful application in content uniformity analysis, dissolution studies and accelerated degradation studies.

Bibliography

1. Lauer HH, Rozing GP. High Performance Capillary Electrophoresis. 2nd ed. Germany: Agilent Technologies; 2018.
2. Whatley H. Basic Principles and Modes of Capillary Electrophoresis. Clinical and Forensic Applications of Capillary Electrophoresis. Pathology and Laboratory Medicine. Humana Press; 2001.
3. EDQM. European Pharmacopoeia. 11th ed. Capillary Eletrophoresis. Strasbourg, Council of Europe: EDQM Publication ID (EPID); 2023.
4. Leach GH. Introduction to Capillary Electrophoresis. Beckman Coulter; 2012.
5. Tagliaro F, Manetto G, Crivellente F, Smith FP. A brief introduction to capillary electrophoresis. Forensic Science International. 1998;92.
6. Petre CF. Principles of capillary electrophoresis. Université Laval; 2007.
7. Skoog D, Holler J, Crouch S. Principles of Instrumental Analysis. 7th ed. Cengage Learning; 2018.
8. Schaeper JP. Reproducibility and optimization in capillary electrophoresis. University of Tennessee; 2002.
9. Kok W. Capillary Electrophoresis: Instrumentation and Operation. Chromatographia CE-Series. 2000;51:36–43.
10. Kelly MA, Altria B' KD, Clark BJ. Approaches used in the reduction of buffer electrolysis effects for routine capillary electrophoresis procedures in pharmaceutical analysis. Journal of Chromatography A. 1997;768.
11. Gagliardi LG, Tascon M, Castells CB. Effect of temperature on acid-base equilibria in separation techniques: a review. Analytica Chimica Acta. Elsevier B.V. 2015;889:35–57.
12. Michałowska-Kaczmarczyk AM, Michałowski T. Dynamic Buffer Capacity in Acid-Base Systems. J Solution Chem. 2015;44(6):1256–66.
13. Morzunova TG. Structure of chemical compounds, methods of analysis and process control capillary electrophoresis in pharmaceutical analysis (a review). 2006;40.

14. Altria K. Improved Performance in Capillary Electrophoresis using Internal Standards. GlaxoSmithKline; 2002.

15. Altria KD, Fabre H. Approaches to Optimisation of Precision in Capillary Electrophoresis. Chromatographia. 1995;40:313–20.

16. Howlett JG. Nebivolol: Vasodilator properties and evidence for relevance in treatment of cardiovascular disease. Canadian Journal of Cardiology. Pulsus Group Inc. 2014;30.

17. Fongemie J, Felix-Getzik E. A Review of Nebivolol Pharmacology and Clinical Evidence. Drugs. 2015;75(12):1349–71.

18. Gupta S, Wright HM. Nebivolol: A highly selective β1-adrenergic receptor blocker that causes vasodilation by increasing nitric oxide. Cardiovascular Therapeutics. 2008;26:189–202.

19. EDQM. European Pharmacopoeia. 11th ed. Nebivolol Hydrochloride Monograph. Strasbourg, Council of Europe: EDQM Publication ID (EPID); 2023.

20. European Medicines Agency. Anexo I – Resumo das Características do Medicamento. In: Nebivolol Aurovitas [Internet]. London: EMA; 2022 [cited 16 September 2023]. Available from: https://extranet.infarmed.pt/INFOMED-fo/pesquisa-avancada.xhtml

21. Ignarro LJ. Different pharmacological properties of two enantiomers in a unique β-blocker, nebivolol. Cardiovasc Ther. 2008;26(2):115–34.

22. Veverka A, Salinas JL. Nebivolol in the treatment of chronic heart failure. Vascular Health and Risk Management. 2007;3.

23. Nebivolol Hydrochloride: Drug Profile. Suresh Gyan Vihar University. Jaipur.

24. Sharma T, Gowrisankar D, Si SC. Extractive Spectrophotometric Determination of Nebivolol Hydrochloride in Pharmaceutical Formulation and Biological Fluids. International Journal of PharmTech Research. 2014; 6.

25. DrugBank Online: Nebivolol. [Internet]. 2007 [cited 15 September 2023]. Available from: https://go.drugbank.com

26. Product Sheet Specifications - GalenIQ™ 721. Beneo-Palatinit GmbH; 2019.

27. Rowe, R.C., Sheskey, P.J., Quinn, M.E. Handbook of Pharmaceutical Excipients. 9th ed. Pharmaceutical Press; 2020.

28. Pharma Excipients Products: GalenIQ 721. [Internet]. 2023 [cited 20 September 2023]. Available from: https://www.pharmaexcipients.com

29. European Medicines Agency. ICH Harmonised Guideline Analytical procedure development Q14. EMA; 2022.

30. European Medicines Agency. ICH Harmonised Guideline Quality risk management Q9. EMA; 2015.

31. European Medicines Agency. ICH Harmonised Guideline Pharmaceutical development Q8(R2). EMA; 2017.

32. Gupta K. Analytical Quality by Design: A Mini Review. Biomed J Sci Tech Res. 2017 Nov 1;1(6).

33. Montgomery DC. Design and Analysis of Experiments. 8th ed. John Wiley & Sons, Inc.; 2012.

34. Czyrski A, Jarzebski H. Response surface methodology as a useful tool for evaluation of the recovery of the fluoroquinolones from plasma-the study on applicability of box-behnken design, central composite design and doehlert design. Processes. 2020 Apr 1;8(4).

35. Belmir H, Abourriche A, Bennamara A, Saffaj T, Ihssane B. Using design space and response surface methodology for developing a liquid chromatography method for simultaneous determination of five statins in pharmaceutical form. Acta Chromatogr. 2021 Dec 1;33(4):345–53.

36. European Medicines Agency. ICH Harmonised Guideline Validation of analytical procedures Q2(R2). EMA; 2022.

37. El-Shafie AS, Yousef A, El-Azazy M. Application of Plackett–Burman Design for Spectrochemical Determination of the Last-Resort Antibiotic, Tigecycline, in Pure Form and in Pharmaceuticals: Investigation of Thermodynamics and Kinetics. Pharmaceuticals. 2022 Jul 1;15(7).

38. H. Fabre, K.D. Altria. Validating CE Methods for Pharmaceutical Analysis. LCGC Europe; 2001.

39. R. M. Ornaf, M. W. Dong. Key concepts of HPLC in pharmaceutical analysis. Handbook of Pharmaceutical Analysis by HPLC; 2005.